Fluidodynamic evaluation of arteriovenous fistulae for hemodialysis

D. LIEPSCH[1], G. PALLOTTI[2], P. PETTAZZONI[3], L. COLÌ[4], G. DONATI[2,4], C. ROSSI[5], F. LOSINNO[5], A. FREYRIE[6], S. STEFONI[2,4]

[1]Laboratory for Fluid Mechanics and Institute for Biotechnology, University of Applied Sciences, Munich - Germany
[2]Department of Clinical Medicine and Applied Biotechnology, University of Bologna
[3]Department of Physics, University of Bologna, Bologna - Italy
[4]Nephrology Dialysis and Renal Transplantation Unit
[5]Department of Radiology
[6]Vascular Surgery Unit, S. Orsola University Hospital, Bologna - Italy

ABSTRACT: Arteriovenous fistulae (AVF) are commonly used in dialysis treatment of uremic patients. However, many AVF create problems and have to be re-examined. Problems arise in the cannulation site and must be treated with antibiotics, and stenosis, both in the arterial and in the venous side of the AVF. In the worst case, the AVF must be replaced for treatment to continue. However, this can only be repeated once before the AVF site is no longer viable. This increases the discomfort, the morbidity and the mortality of the dialysis patient. Several kinds of AVF were studied to determine whether flow disturbances give rise to these complications. Many studies have already demonstrated the importance of hemodynamic factors in vascular disease pathogenesis. These factors include: the pulsatility of flow, the elasticity of the vessel, the non-Newtonian blood, flow behavior and, very importantly for AVF, the vessel geometry. In model studies, intimal changes have been observed in bends and bifurcations, regions of vessel construction and vessel stenosis. In these regions, blood flow changes abruptly and this contributes to arterial disease. We prepared several one-to-one, true-to-scale elastic silicon rubber models of different AVF. The AVF models were based on angiographic studies of chronic dialysis patients and on AVF from the arms of cadavers. The models had a similar compliance to that of the human blood vessel. Flow was visualized using photoelasticity apparatus and a birefringent blood-like fluid. This method is suitable to analyze the spatial configuration of flow profiles, to differentiate laminar flow from disturbed flow, and to visualize flow separation, vortex formation and secondary flow. It was found that AVF create disturbances that are not found under normal physiological flow conditions. The X-formed AVF was very unsatisfactory, creating significant flow disturbances. The AVF had high velocity fluctuations. These could lead, for example, to aneurysm formation. A better configuration would be an end-to-end AVF. However, this formation creates other complications. For example, there is not enough blood to the hand and parts of the hand lose feeling. The recommended AVF would be an end-to-side anastomosis. In this case, attention is needed for placement geometry, to minimize additional flow disturbances. Several models as well as patient angiographic studies are discussed. (The Journal of Vascular Access 2003; 4: 92-7)

KEY WORDS: *Fluidodynamics, Models, Birefringent set-up, Arteriovenous fistulae, Hemodialysis*

INTRODUCTION

Constructing vascular access (VA) for extracorporeal hemodialysis (HD) is a key procedure in this life-saving therapy for uremic patients. VA must guarantee the blood-flow for the dialyzer to perform its depurative efficacy and must be easy to operate. It has also been shown to be one of the main causes of direct and indirect clinical complications: it is the prime cause of hospitalization in the early months of artificial replacement therapy and also affects the uremic patient's general morbidity in
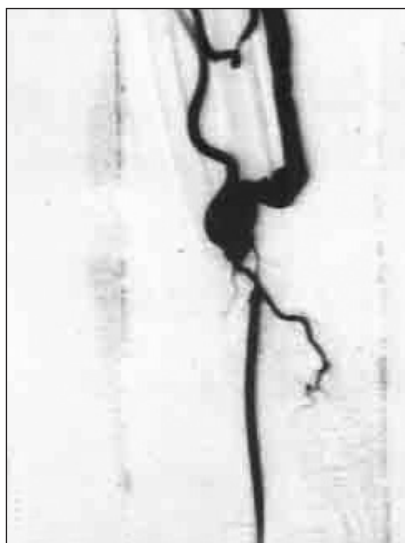
Fig. 1 - *Angiography of the radial artery.*

Fig. 2 - *Silicon rubber model prepared from the angiogram.*

the medium and long term (1).

Cimino and Brescia devised the first type of VA in 1964. They constructed an arteriovenous fistula (AVF) between the radial artery and the cephalic vein in the arm. Current surgical techniques afford a number of VA for HD, the timing and choice being geared to preserving and protecting the vascular site as far as possible.

In the case of early referral uremic patients, there is time to devise the correct vascular approach, setting up distal radio-cephalic fistulae, preferably in the non-dominant arm, with a latero-terminal arterio-venous anastomosis. When this approach is technically unfeasible, it is preferable to resort to a brachio-cephalic fistula at the bend of the elbow (latero-lateral anastomosis). Occasionally the patient's venous site is so impaired as to need a prosthesis segment implant (generally polytetrafluoroethylene (PTFE)) in the arm (straight omero-axillary segments) or the thigh (femoro-femoral loop).

Late referral is becoming common, when renal function has completely failed and artificial replacement is urgent. In such patients, it is necessary to resort to venous catheters, which can be used immediately. This access carries with it a high risk of thrombotic or infections complication and often causes stenosis of the insertion vein resulting in permanent damage.

The most widely used VA still in use today is the distal radio-cephalic AVF. This VA has an average life span of 2-3 years; its main complication is post-anastomotic venous stenosis, which generally develops in the first few months after creation and can be further complicated by stenotic segment thrombosis. One of the main causes of this complication is blood turbulence when passing through the anastomosis and crossing the first segment immediately after it.

Research into the fluidodynamics of this fistula using *in vitro* simulated models shed light on why this type of VA is prone to stenotic and thrombotic complications: calibre differences between anatomized vessels, the angle of alignment of the vein to the artery, breadth of anastomosis, etc (2-6). Such *in vitro* observations can be used to improve the technique of construting this fistula, therefore, cutting down the medium and long-term complications.

MATERIALS AND METHODS

Models

We constructed models based on patient angiograms. However, the exact geometry differs slightly from the actual vessel. In addition to the models constructed by this method, AVF with an arteriotomie length of 1 cm were obtained from the lower arm of cadavers. These fistulae were then filled with silicon. The silicon casts were used to prepare forms. These forms were filled with wax and the resulting wax cast was dipped in transparent silicon rubber several times. Finally the wax was melted out and a transparent silicon rubber model was obtained that had the exact size and shape and a similar compliance to the original vessel. This technique had the advantage that several models can be prepared with the exact same geometry and the experiments are directly reproducible (7).

We studied five AVF models: an end-to-side anastomosis with a sharp angle, an end-to-side anastomosis with a wide angle, a side-to-side anastomosis, an end-to-end anastomosis and an end-to-side anastomosis from an angiogram.

The fifth model was prepared from an angiogram
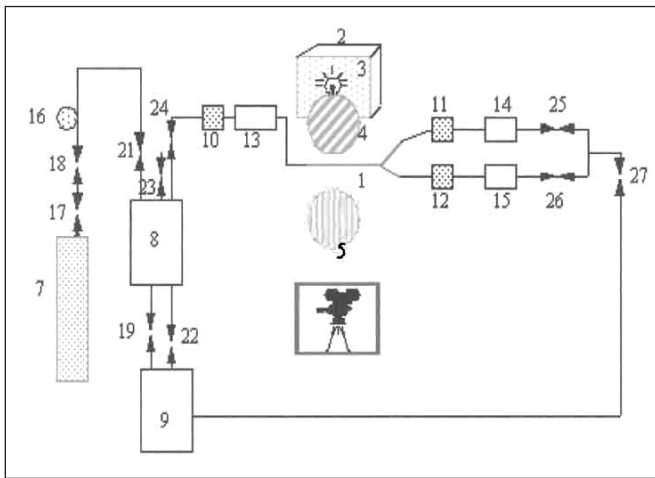
Fig. 3 - *Birefringent solution set-up, methods. 1) Model; 2) Lampbox; 3)Screen; 4) Polfilter; 5) Analyzer; 6) Camera; 7) N-bottle; 8) Storage Box; 9) Collector; 10-12) Pressure controller; 13-15) Flowmeter; 16) Pressure-meter; 17-27) Ventil Spherical Faucet.*

Fig. 4 - *End-to-side anastomosis with a birefringent solution. The light field demonstrates high velocity fluctuations. Entrance flow was 300 ml/min, into the hand 30 ml/min.*

showing blood flow through the radial artery connected to the cephalic vein with a 180° bend (Fig. 1). This angiogram model was prepared using wax from the AmniDent Co. This wax has a melting point of 58° C.The wax model (Fig. 2) was painted with a protective film, SF18 (Wacker Co).The silicon for the model was then prepared by mixing Elastonsil RT 601A with a hardener (RT601B) with a ratio of 9:1. To avoid air bubbles in the model, the silicon was placed in a vacuum chamber and the air removed. The wax cast was immediately dipped into the prepared silicon and dried for at least 1 hr. The wax cast was dipped seven times to ensure the correct wall thickness. The wax was then melted out in an oven at approximately 100° C and cleaned with isopropanol.

The study followed the principles outlined in the Declaration of Helsinki.

Flow visualization

The flow was visualized at a steady flow using dyes. The birefringent technique was used to obtain additional information, as the complete flow field can be observed at pulsatile flow. With dyes this is not possible and only single stream paths can be seen. A further advantage of using a birefringent solution and photoelasticity apparatus is that the entire length of the disturbed area is visible. This includes the flow separation and reattachment points and the location and extent of the reverse flow in the flow separation region. The method has been previously explained (8). The birefringent fluid was a vanadium pentoxide water solution.

Experimental set-up

We studied the flow at different flow rates with Re = 250, Re = 500 and Re = 1000 and a flow rate ratio of 70:30 for the end-to-side models. Figure 3 shows the experimental set-up. At steady flow, the fluid was pressed into the model with nitrogen. The flow ratio was regulated by precision valves and measured with flowmeters. A pump (Reul et al) created a pulsatile flow and a buffer tank was installed between the heart pump and three pressure transducers. Systolic pressure was maintained at approximately 120 mmHg and diastolic pressure at approximately 80 mmHg. The pressure was measured with inductive pressure transducers (Hottinger, Darmstadt, Germany). The pressure tranducers were installed in a straight plexiglass tube with a diameter of 9.1 mm at a distance of 1 m from each other, proximal to the model. The unsteady pressure $p(t)$ was measured at two points 1 m apart and their difference recorded to yield dp/dx. For pulsatile flow, it was necessary to install buffer tanks between the flowmeters and the models.

RESULTS

The flow in the different models was studied at various flow rates and flow rate ratios as demonstrated by the following figures. All flow studies were recorded on videotape. Figure 4 shows an end-to-side anastomosis with a sharp bifurcation angle and an entrance Reynolds number of approximately 1000 (~ 300 ml/min). The flow, from left to right,
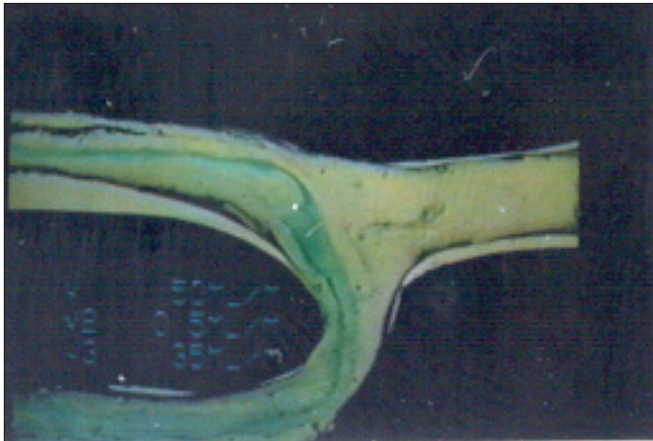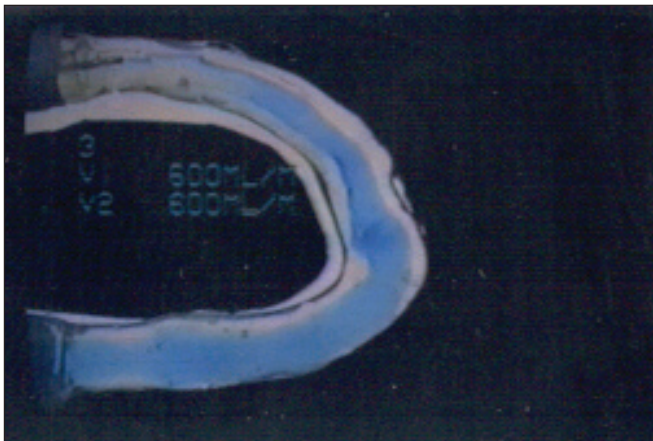
Fig- 5 - *End-to-side anastomosis with a wide bifurcation angle. The green dye shows slight velocity disturbances.*

Fig. 6 - *End-to-side anastomosis with wide bifurcation angle with a birefringent solution. The entrance flow as 900 ml/min into the hand 90 ml/min.*

Fig. 7 - *End-to-end anastomosis with a blue dye.*

Fig. 8 - *End-to-end anastomosis with birefringent solution.*

contains a black line in the centre at the entrance. High velocity fluctuations are visible at the bifurcation and in the branch, shown as a large white area. Very high velocity fluctuations are present demonstrated by various laser-Doppler-anemometer measurements.

Figure 5 shows an end-to-side anastomosis with a wide, smooth bifurcation angle. It is clearly visible that the green dye spreads out across the flow field caused by the normal flow in a bend. However, the flow is very calm with few vortices and no additional vortex formation at the bifurcation. Figure 6 shows the same anastomosis with a birefringent solution. The white area in the bend is due to the secondary flow typical of every bend and bifurcation. The flow at the bifurcation is calm compared to the end-to-side anastomosis with a sharp bifurcation angle shown in Figure 4.

The end-to-end anastomosis (Fig. 7) produces a very calm flow even at higher Reynolds numbers (up to 2000). The stream path of the blue dye hits the wall at the bend and spreads out over the whole cross-section due to the secondary flow. Similar flow behavior is visible with a birefringent solution (Fig. 8). High velocity disturbances are created with the side-to-side anastomosis (Fig. 9). The blue dye in the centre spreads out over the whole area at the bifurcation and distal to the bifurcation. Such AVF create very high velocity fluctuations clearly visible on the video. (We also studied AVF in rabbits and found velocity fluctuations of up to 1500-2000 Hz with amplitudes that were approximately 80% of the normal pulse, Fig. 10. Therefore, in humans up to 500 Hz can be reached). Such velocity frequencies may damage the vessel wall. They produce a hammer effect (6) forming aneurysms. From pre-
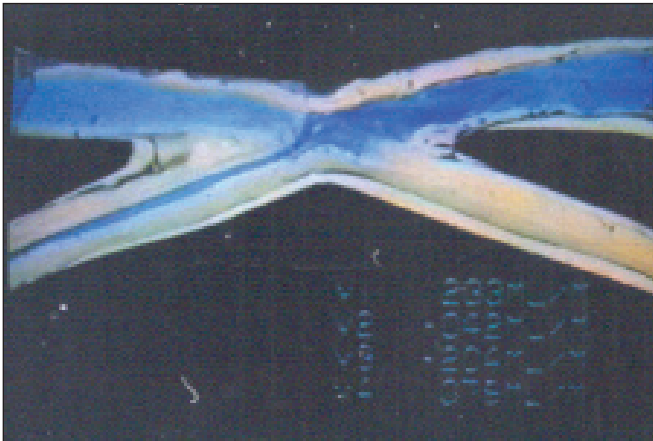
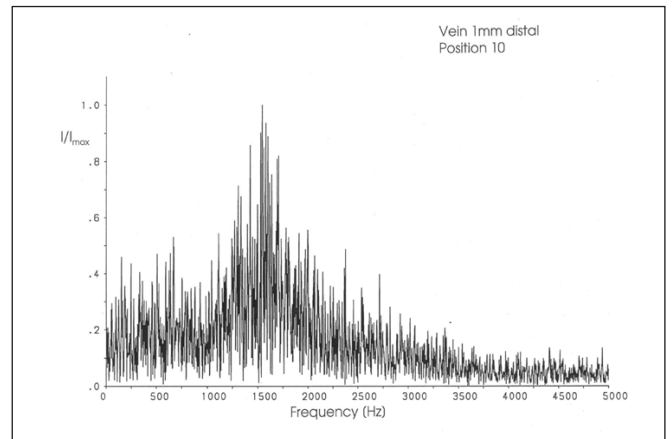**Fig. 9** - *Side-to-side anastomosis with a blue dye.*

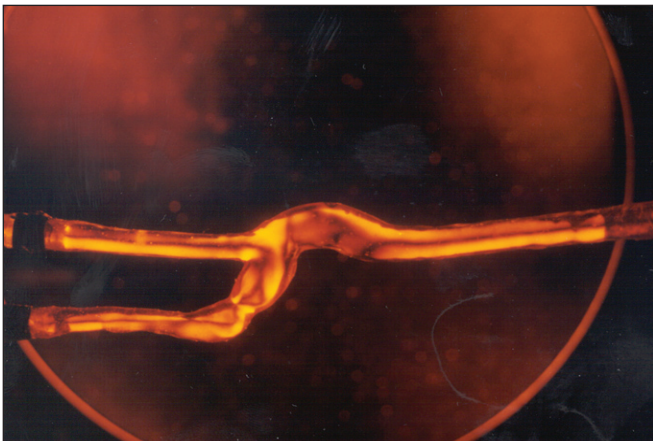**Fig. 10** - *Velocity fluctuations in a side-to-side anastomosis measured with a laser vibrometer in a rabbit.*

Fig. 11 - *Angiogram model with birefringent solution entrance Re number = 250. Flow rate ratio V3/V1 = 70/30.*
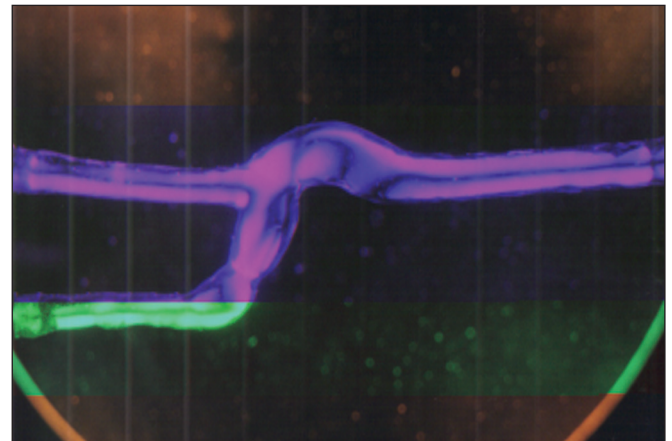

Fig. 12 - *Same as Figure 11, but Re = 500, V3/V1 =70/30.*

liminary studies (7) we concluded that the end-to-end anastomosis produced the smoothest flow behavior.

The end-to-side anastomosis with a wide angle also shows a relatively calm flow behavior compared with the other two models.

In the model prepared from the angiogram (Figs. 11 and 12) the flow is slightly disturbed at the bifurcation; however the black line returns to the centre of the tube after having passed the bifurcation. At the bifurcation, several black lines are visible. These indicate the creation of a higher order of isochromates demonstrating higher shear stresses and higher velocity disturbance. With a higher Reynolds number the velocity fluctuations increase forming several flow separation regions. Therefore, the flow should be low, so that no additional complications are created, i.e. stenosis or aneurysm formation.

DISCUSSION

The importance of the flow field at bends and bifurcations has already been demonstrated experimentally and numerically (9-11). Zheng presented an overview of the many studies in bifurcations up until 1992 (12). The geometry of the anastomosis is obviously of great interest because AVF restenosis with a total blockage is common. Earlier fundamental studies (13) showed that the side-to-side anastomosis and the end-to-side anastomosis with a sharp angle produced a flow field with high velocity fluctuations, vortex formation and high shear stress areas. Any of these can create physicochemical reactions causing thrombocyte activation and forming micro-thromboses and agglomeration in low shear regions. The flow turns towards the wall at the bend and this creates higher local pressure at

the wall (stagnation zone). In turn this can produce a post-operative aneurysm as the vein wall is very thin. Therefore, stagnation points at the vein wall must be considered as important. Studies already published (14) show the high and low shear gradient influence. From these studies, it is well known that intimal changes occur predominantly in specific vessel segments such as bends and bifurcations. Even relatively low shear stresses can change the endothelial layer or injure the endothelial cells. Therefore, it is essential to avoid additional velocity fluctuations with high frequencies.

We could show that the end-to-side anastomosis with a wide bifurcation angle and the end-to-end anastomosis significantly reduce high velocity gradients and stagnation points. In contrast to the other two models, there were no high shear stresses in these two models. The angiogram model results fall in between the end-to-side model with a wide angle and that with the sharp angle. The low flow (Reynolds <300) showed no extreme re-circulation zones with high velocity fluctuations. However, with increasing velocities, stronger velocity fluctuations with several flow separation regions were observed. It is important to minimize these effects otherwise the velocity fluctuations can lead to an aneurysm. Therefore, the end-to-side anastomosis with a wide

bifurcation angle and the end-to-end anastomosis are the best choices for an orthotopic AVF, depending on the anatomy. Earlier studies used different fistula lengths of an adjunctive AVF in the distal anastomosis of a femoro-femoral PTFE arteriovenous graft. We found that the widest fistula is the best in terms of biofluid dynamics (15), because the velocity fluctuations are much smaller than in the smaller fistula sites where a rough flow pattern was observed.

ACKNOWLEDGEMENTS

Address for correspondence:
Prof. Sergio Stefoni
Nephrology Dialysis and Renal Transplantation Unit
S.Orsola University Hospital
Via Massarenti 9
40138 Bologna, Italy
sergio.stefoni@unibo.it

REFERENCES

1. Arora P, Kausz AT, Obrador GT, Ruthazer R, Khan S, Jenuleson CS et al. Hospital utilization among chronic dialysis patients. J Am Soc Nephrol 2000; 11: 740-6.
2. Caro CG. Arterial fluid mechanics and atherogenesis. Recent advances in cardiovascular Disease 1981; II: 6-11.
3. Fry DL. Acute vascular endothelial changes associated with increased blood velocity gradients. Circ Res 1968; 22: 165-97.
4. Nerem RM. Arterial fluid dynamics and interactions with the vessel walls. In: Schwartz DJ, Werthessen, NT, Wolf S eds. Structure and function of the circulation 2. New York: Plenum Publishing Corp 1981; 719-835.
5. Sottinrai VS, Lim Sue S, Feinberg EL, Bringaze WL, Tran AT, Batson R. Distal anastomotic intimal hyperplasia: Biogenesis and etiology. Eur J Vasc Surg 1998; 2: 245-56.
6. Stehbens WE, Liepsch DW, Poll A, Erhardt W. Recording of unexpectedly high frequency vibrations of blood vessel walls in experimental arteriovenous fistulae of rabbits using a laser vibrometer. Biorheology 1995; 32: 631-41.
7. Liepsch DW, Moravec ST, Baumgart R. Some flow visualization and laser-Doppler-velocity measurements in a true-to-scale elastic model of a human aortic arch-a new model technique. Biorheology 1992; 29: 563-80.
8. Liepsch D, Poll A, Strigberger J, Sabbah HN, Stein PD. Flow visualization in a mold of the normal human aorta and renal arteries. J Biomech Eng 1989; 3: 222-7.
9. Karino T. Mikroskopische Struktur der gestörten Strömung im arteriellen und venösen System, sowie deren Bedeutung für die Kokalisation von Gefäuerkrankungen. Hämostaseologie 1991; 22: 30-3.
10. Perktold K, Rappitsch G. Mathematical modeling of arterial blood flow and correlation to atherosclerosis. Technol Health Care 1995; 3: 139-51.
11. Reneman RS, Van Merode T, Hick P, Hoeks APG. Flow velocity patterns and distensibility of the carotid artery bulb in subjects of various ages. Circulation 1985; 71: 3: 500-9.
12. Zheng Lou, Yang Wen-Ji. Biofluid dynamics at arterial bifurcations. Crit Rev Biomed Eng 1992; 19: 455-93.
13. Maurer PC, Pflugbeil G, Rieger D, Liepsch D, Wahba A. Update on the role of arteriovenous fistulas in distal bypass operations: Visualization of flow patterns in transparent models. In Frank J. Veith ed. Current critical problems in vascular surgery. St. Louis, Missouri: Quality Medical Publishing Inc 1992; 87-97.
14. Yoshida Y, Yamaguchi T, Caro CG, Glagov S, Nerem RM. Role of blood flow in atherogenesis. Tokyo: Springer 1988.
15. Pflugbeil G, Liepsch D, Tröster J, Kurz G, Maurer PC. Fluiddynamische Studien zur speziellen Hämodynamik in der Brescia-Cimino Fistel. Angio 1994; 16: 177-122.